Dexterous Manipulation Planning and Execution of an Enveloped Slippery Workpiece

J.C. Trinkle
Dept. of CS

R.C. Ram
Dept. of EE

A.O. Farahat
Dept. of AE

P.F. Stiller
Dept. of Math

Texas A&M University, College Station, TX 77843

Abstract

Robotic hands or arms that are capable of enveloping the workpieces that they manipulate hold several advantages over mechanism that cannot. One important advantage is that envelopment of the workpiece ensures grasp maintenance even if the object experiences significant external forces in directions unknown prior to grasp synthesis. This makes enveloping mechanism useful in low-friction and microgravity environments. In this paper we define first-order stability cells which were used to plan a planar, "whole-arm," manipulation task of a slippery workpiece. For most, but not all, of the plan, the workpiece was enveloped. Experimental results are presented.

1 Introduction

Robotic manipulation systems (e.g., hands and multi-arm systems) that are capable of enveloping the workpieces that they manipulate can execute "power grasps" from which the workpiece cannot be removed without displacing, perhaps even bending, the mechanism's links. This type of grasp is particularly useful when manipulation takes place in low friction or microgravity environments. Envelopment, however, requires at least $n_q + 1$ contacts between the workpiece and manipulation system, where n_q is the number of degrees of freedom of the uncontacted workpiece. Thus envelopment using only finger tips is impractical. Instead, all surfaces of all of the links of the manipulator system should be used [10]. This concept is referred to as "whole-arm" manipulation [9]. When not restricting contacts to be on the finger tips, manipulation of an enveloped workpiece can be achieved by systems with small numbers of links and actuators, thereby reducing the mass and complexity of the mechanism. This reduced complexity results in lost dexterity which must be recaptured (to the extent possible) by allowing contact sliding. However, there have been relatively few studies addressing the issues raised by allowing contacts on any surface of any link and still fewer which also address issues associated with sliding.

In this paper, we consider the quasistatic, "whole-arm," dexterous manipulation of slippery workpieces. Task planning is achieved by cell decomposition of the system's configuration space, or C-space, first into contact formation cells, or CF-cells, from which first-order stability cells, or FS-cells, are generated. CF-cells are patches of "contact space" used to delineate the boundaries between "free space" and "obstacle space." We introduce FS-cells, which are the physical counter parts of CF-cells. Their use in planning ensures that all plans found satisfy the applicable geometric restrictions and physical constraints. A simple, planar, manipulator system with two actively controlled links was constructed to execute whole-arm, dexterous manipulation plans. Experimental results of a plan consisting of enveloping and nonenveloping manipulation segments are presented.

1.1 Related Work

The work reported on here is unique in that a workpiece was reoriented within a mechanical articulated hand using the surfaces of the fingers and palm. The object was slippery with an effective coefficient of friction approximately equal to 0.1. If the coefficient had been larger than 0.15, the plan would have failed due to jamming.

There are several closely related research efforts that have played a role in motivating this work. In particular, both Fearing [3] and Brock [1] realized the importance of sliding in the enhancement of dexterity. While contacts were restricted to the finger tips, they used the Salisbury Hand to perform manipulation tasks with sliding. Other closely related work has been done by Mason [7], Peshkin [8], and Lynch [6] on the motion of a workpiece sliding in a horizontal plane with single and multiple points of contact and an unknown externally applied wrench. Relevant research has been reported in the mechanisms literature in the area of closed-loop serial linkages, but few models treat contact friction and the quasistatic case considered here.

2 Problem Statement

Given the initial and goal configurations of a manipulator system and a workpiece (see Figure 1), dexterous manipulation planning is the act of determining joint angle and joint effort trajectories which, if executed, would effect the desired change of configuration. In studying this problem, we have made the

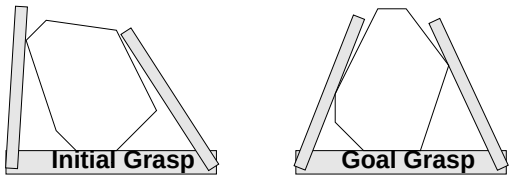

Figure 1: Initial and goal configurations.

following assumptions: each body in the system is a rigid polyhedron; dynamic effects are negligible; the geometry of each body in the system is known; the external load acting on each body is known; and each joint's controller may operate in a position-control or effort-control mode may be switched during manipulation.

Since dynamic effects are assumed to be negligible, the motion of the system depends entirely on the set of kinematic constraints applicable at each instant. Let $\dot{\mathbf{q}}$ and $\dot{\theta}$ be the generalized velocity vectors of the workpiece and the manipulator system, respectively, with lengths n_q and n_θ . Then the applicable kinematic constraints can be written as follows [14]:

$$\mathbf{W}_A^T \, \dot{\mathbf{q}} \; - \mathbf{J}_A \, \dot{\theta} \; = \mathbf{0} \tag{1}$$

where each row of the transposed applicable wrench matrix $\mathbf{W}_A^T$ and the applicable Jacobian matrix $\mathbf{J}_A$ correspond to one applicable kinematic constraint on the system. For each sliding contact, equation (1) ensures that the normal relative velocity at the contact is zero. For each rolling contact, both the normal component of relative velocity and the tangential component are zero. Thus we see that $\mathbf{W}_A^T$ and $\mathbf{J}_A$ have $2n_R + n_S$ rows, where n_R and n_S are the numbers of rolling and sliding contacts, respectively. Equation (1) only applies to sliding and rolling contacts. All other contacts must break. This condition can be written as the following system of linear inequalities:

$$\mathbf{W}_{nB}^T \dot{\mathbf{q}} - \mathbf{J}_{nB} \dot{\theta} > \mathbf{0} \tag{2}$$

where the left-hand side of the inequality represents the normal components of the relative velocities at the contacts presumed to be breaking.

Since dynamics effects are negligible, the system is quasistatic and therefore must satisfy the following equilibrium equations and Coulomb friction constraints at every instant:

$$\mathbf{W}_{A\mu} \; \mathbf{c}_A \;\; = \;\; -\mathbf{g}_{ext} \tag{3}$$

$$\mathbf{J}_{A\mu}^T \; \mathbf{c}_A \;\; = \;\; -\mathbf{G} \; + \boldsymbol{\tau} \tag{4}$$

$$\mathbf{B}_A \; \mathbf{c}_A \;\; > \;\; \mathbf{0}. \tag{5}$$

Here $\mathbf{c}_A$ is the applicable vector of wrench intensities, $\mathbf{g}_{ext}$ is the external wrench applied to the workpiece, $\boldsymbol{\tau}$ is the vector of joint efforts, and $\mathbf{G}$ is the vector joint efforts induced by external loads acting on the manipulator system. The matrices $\mathbf{W}_{A\mu}$ and $\mathbf{J}_{A\mu}$ are slightly modified versions of $\mathbf{W}_A$ and $\mathbf{J}_A$ that reflect the fact that for sliding contacts, the tangential components of the contact forces are proportional to the normal components. It is important to note that these matrices depend on the values of $\dot{\theta}$ and $\dot{\mathbf{q}}$, so that the kinematic and equilibrium equations are coupled. If the workpiece is frictionless or if all contacts are rolling, $\mathbf{W}_{A\mu}$ and $\mathbf{J}_{A\mu}$ are identical to $\mathbf{W}_A$ and $\mathbf{J}_A$, respectively. Inequality (5) ensures that the contact forces at rolling contacts lie within their Coulomb friction cones and all contact forces are compressive. The matrix $\mathbf{B}_A$ becomes the identity matrix if all contacts are sliding or if the object is frictionless (see [14] for more details).

Accurate motion prediction is only possible if the set of applicable kinematic constraints can be identified at every instant. Unfortunately there may be more that one feasible set for a given configuration [14]. Therefore, in planning quasistatic manipulation tasks, we are forced to consider 3^{n_c} sets of applicable kinematic constraints, where n_c is the number of contacts. Henceforth, the motion associated with each set will be referred to as a *mode of motion*.

3 Planning and Execution

Our approach to planning dexterous manipulation tasks involving slippery workpieces is broken into two phases. In Phase 1, frictionless planning proceeds via a CF-cell [13] decomposition of C-space. The CF-cells are modified to create FS-cells whose connectivity is represented in a graph. A path through the graph connecting the nodes corresponding to the initial and goal configurations defines a family of usable joint trajectories. However, these trajectories are only correct in the absence of friction. A side effect of planning under the frictionless assumption is that all contacts are presumed to slide. Attempting to execute the plan in an environment with friction may fail if any of the contacts roll. The results of Phase 2 are trajectory modifications that prevent the occurrence of rolling contact.

3.1 Planning: Phase 1

Phase 1 relies on the decomposition of C-space into contact formation cells, portions of which are subsequently identified (and augmented if necessary) to generate stability cells. Stability cells are particularly useful in the frictionless case, because all paths within them correspond to reversible quasistatic motions [13].

3.1.1 Contact Formation Cells

A contact formation, or CF, [2] is a qualitative representation of the state of contact among all the bodies in the system. A CF is conveniently viewed as a list

of elemental contacts (vertex-face and edge-edge contacts), that corresponds to a surface patch of a configuration obstacle, or C-obstacle (for examples of CF's see [2] and [11]). A contact formation cell, or CF-cell, is the set of points, $(\mathbf{q}\ ,\boldsymbol{\theta}\ )$, in C-space for which a particular set of elemental contacts is achieved and no bodies interpenetrate. Let ec be a set of elemental contacts and let $\mathcal{EC}$ be the set of configurations for which the elemental contacts specified by ec are satisfied without regard for interference between bodies in the system at points away from the specified elemental contacts. The set $\mathcal{EC}$ can be written as follows:

$$\mathcal{EC} = \{(\mathbf{q}\ ,\boldsymbol{\theta}\ ) \mid \mathbf{f}_{geo} = \mathbf{0} \bigwedge \mathbf{h}_{geo} > \mathbf{0}\} \qquad (6)$$

where $\mathbf{q}$ and $\boldsymbol{\theta}$ represent the configurations of the workpiece and manipulation system, respectively. The elements of the vector functions $\mathbf{f}_{geo}$ and $\mathbf{h}_{geo}$ are C-functions defined in [4]. Since the elements of $\mathbf{f}_{geo}$ represent geometric constraints, they will be referred to as geometric C-functions. The maintenance of the equation $\mathbf{f}_{geo} = \mathbf{0}$ guarantees for edge-edge and face-vertex contacts that the lines supporting the edges intersect and the vertices lies in the planes supporting the faces, respectively. They do not guarantee that the points of contact lie within the finite bounds of the edges and faces of concern. These constraints are represented by the inequality $\mathbf{h}_{phy} > \mathbf{0}$. However, they do not prevent the overlapping of feature pairs other than those in the current set of elemental contacts. Therefore, $\mathcal{EC}$ must be intersected with $\mathcal{C}_{valid}$, defined by Latombe to be the union of free space and contact space [4]. The set $\mathcal{CF}$ contains all system configurations which are geometrically feasible for a given set of elemental contacts. The vector function $\mathbf{f}_{geo}$ has one element for every elemental contact. While any number of elemental contacts is possible, in most manipulation scenarios involving sliding contacts, there will be less than $n_q + n_\theta$ contacts. The satisfaction of more than $n_q + n_\theta$ geometric C-functions would require special part geometries.

3.1.2 First-Order Stability Cells

In this section, the stability constraints, or physical C-functions, are derived as functions of $\mathbf{q}$, $\boldsymbol{\theta}$, and the joint effort vector, $\boldsymbol{\tau}$. We make use of the following relationships [13]:

$$\mathbf{W}_n^T = \frac{\partial \mathbf{f}_{geo}}{\partial \mathbf{q}} \qquad \mathbf{J}_n = -\frac{\partial \mathbf{f}_{geo}}{\partial \boldsymbol{\theta}} \qquad (7)$$

where $\mathbf{J}_n$ and $\mathbf{W}_n^T$ are the Jacobian and transposed wrench matrices corresponding to the normal components of the relative velocities at all contact points. Note that if all contacts are sliding (which is normally the case when the workpiece is frictionless), then $\mathbf{W}_n$ and $\mathbf{J}_n$ are identical to $\mathbf{W}_A$ and $\mathbf{J}_A$, respectively.

First-order stability requires that the wrench matrix, $\mathbf{W}_n$, have full row rank and that there exist at least n_q strictly positive elements of the wrench intensity vector, $\mathbf{c}_n$, an n_c-vector [12]. Under these restrictions, $\mathbf{W}_n$ can always be written as $[\mathbf{W}_{nI} \mid \mathbf{W}_{nII}]$ such that $\mathbf{W}_{nI}{}^{-1}$ exists. The wrench intensity vector is then given by:

$$\mathbf{c}_n\ (\mathbf{q}\ ,\boldsymbol{\theta}\ ,\mathbf{k}\ ) = (\mathbf{s}\ + \mathbf{H}\ \mathbf{k}\ )/d\ ;\ \ d \neq 0 \qquad (8)$$

where d, $\mathbf{s}$, and $\mathbf{H}$ are defined below:

$$\mathbf{s}\ (\mathbf{q}\ ,\boldsymbol{\theta}\ ) = \begin{bmatrix} -Adj(\mathbf{W}_{nI}\ )\mathbf{g}_{ext} \\ \mathbf{0} \end{bmatrix} \qquad (9)$$

$$\mathbf{H}\ (\mathbf{q}\ ,\boldsymbol{\theta}\ ) = \begin{bmatrix} -Adj(\mathbf{W}_{nI}\ )\mathbf{W}_{nII} \\ \mathbf{I} \end{bmatrix} \qquad (10)$$

$$d(\mathbf{q}\ ,\boldsymbol{\theta}\ ) = Det(\mathbf{W}_{nI}\ ) \qquad (11)$$

where Adj and Det are the adjoint and determinant operators, $\mathbf{k}$ is an arbitrary positive vector of length η whose elements are the internal wrench intensities [7], and $\mathbf{I}$ is the identity matrix. The scalar η is the nullity of $\mathbf{W}_n$ and can be viewed as the number of "extra" contacts which must be maintained by compliant control. In the frictionless case, the Coulomb friction model does not apply. We simply restrict the wrench intensity vector to have strictly positive elements. Applying this condition to equation (8) yields the following physical C-function constraint applicable to first-order stability cells:

$$\mathbf{h}_{phy}\ (\mathbf{q}\ ,\boldsymbol{\theta}\ ,\mathbf{k}\ ) = (\mathbf{s}\ + \mathbf{H}\ \mathbf{k}\ )/d > 0\ ;\ \ d \neq 0. \qquad (12)$$

The elements of the internal wrench intensity vector $\mathbf{k}$ cannot be uniquely represented in C-space. Therefore, C-space could be augmented by the elements of $\mathbf{k}$. Since these elements are not directly controllable, we relate them to $\boldsymbol{\tau}$ and augment C-space with its elements. Substituting equation (8) into equation (4) and rearranging yields:

$$(\boldsymbol{\tau}\ - \mathbf{G}\ )d - \mathbf{J}_n^T\ \mathbf{s}\ = \mathbf{J}_n^T\ \mathbf{H}\ \mathbf{k}\ \ ;\ \ d \neq 0. \qquad (13)$$

In most situations, there will be at least as many joints as "extra" contacts (i.e., $n_\theta \geq \eta$) and the product $\mathbf{J}_n^T\ \mathbf{H}$ will be full rank. Denoting $\mathbf{J}_n^T\ \mathbf{H}$ by the $(n_\theta\ \times \eta)$ matrix $\mathbf{A}$, rearranging its rows, and partitioning it such that $\mathbf{A}_{\ I}$ is nonsingular yields: $\mathbf{A}\ = \begin{bmatrix} \mathbf{A}_{\ I} \\ \mathbf{A}_{\ III} \end{bmatrix}$. Equation (13) can now be solved for $\mathbf{k}$ to yield[1]:

$$\mathbf{k}\ (\mathbf{q}\ ,\boldsymbol{\theta}\ ,\boldsymbol{\tau}\ ) = \mathbf{A}_{\ I}^{-1}[(\boldsymbol{\tau}_{\ I} - \mathbf{G}_{\ I})d + (\mathbf{J}_n^T\ \mathbf{s}\ )_I]\ ;\ \ d \neq 0 \qquad (14)$$

where $\boldsymbol{\tau}_I$, $\mathbf{G}_I$, and $(\mathbf{J}_n^T\ \mathbf{s}\ )_I$ are the partitions of $\boldsymbol{\tau}$, $\mathbf{G}$, and $(\mathbf{J}_n^T\ \mathbf{s}\ )$ corresponding to the partition $\mathbf{A}_{\ I}$. The $n_\theta - \eta$ equations of the manipulator system corresponding to the partition $\mathbf{A}_{\ III}$ have not yet been used, but must also be satisfied for equilibrium. They give rise to $\mathbf{f}_{phy}$ which is defined as follows:

$$\mathbf{f}_{phy}\ (\mathbf{q}\ ,\boldsymbol{\theta}\ ,\boldsymbol{\tau}\ ) = \mathbf{A}_{\ III}\mathbf{k}\ + (\mathbf{G}_{\ III} - \boldsymbol{\tau}_{\ III})d + (\mathbf{J}_n^T\ \mathbf{s}\ )_{III}\ ;\ \ d \neq 0 \qquad (15)$$

[1] The case for which $\mathbf{A}$ does not have full column rank can be handled similarly (see [13] for details).

where $\boldsymbol{\tau}_{III}$, $\mathbf{G}_{III}$, and $(\mathbf{J}_n^T\ \mathbf{s}\ )_{III}$ are the partitions of $\boldsymbol{\tau}$, $\mathbf{G}$, and $(\mathbf{J}_n^T\ \mathbf{s}\ )$ corresponding to the partition $\mathbf{A}_{III}$. Note that because $\mathbf{A}_I$ is nonsingular, it provides a one-to-one and onto mapping relating $\mathbf{k}$ and $\boldsymbol{\tau}_I$, thus allowing complete control over the internal wrench intensities.

We are now in a position to define first-order stability cells, or FS-cells, in the augmented, $n_q + 2n_\theta$-dimensional C-space. For a given CF-cell, only the points satisfying equations (3) and (4) and inequality (5) are members of the corresponding FS-cell, $\mathcal{FS}$, which is defined as follows:

$$\mathcal{FS} = \mathcal{CF} \cap \mathcal{S} \tag{16}$$

where $\mathcal{S} = \mathcal{S}^+ \cup \mathcal{S}^-$ and $\mathcal{S}^+$ and $\mathcal{S}^-$ are defined as follows:

$$\begin{aligned} \mathcal{S}^+ &= \{(\mathbf{q}\ ,\boldsymbol{\theta}\ ,\boldsymbol{\tau}\ ) \mid \mathbf{f}_{phy}\ = \mathbf{0} \bigwedge \mathbf{k}\ > \mathbf{0} \\ &\quad \bigwedge \mathbf{s}\ + \mathbf{H}\ \mathbf{k}\ > \mathbf{0} \bigwedge d > 0\} \qquad (17) \\ \mathcal{S}^- &= \{(\mathbf{q}\ ,\boldsymbol{\theta}\ ,\boldsymbol{\tau}\ ) \mid \mathbf{f}_{phy}\ = \mathbf{0} \bigwedge \mathbf{k}\ < \mathbf{0} \\ &\quad \bigwedge \mathbf{s}\ + \mathbf{H}\ \mathbf{k}\ < \mathbf{0} \bigwedge d < 0\} \qquad (18) \end{aligned}$$

Equation (15) suggests two classes of FS-cells: compliant and noncompliant. It should be clear, however, that in all configurations, the workpiece will comply passively with the motion of the manipulator system. What is meant by compliance here, is active compliance of the manipulator system. The noncompliant class of FS-cells is characterized by the nonsingularity of $\mathbf{W}_n$ and the maintenance of n_q contacts. The most important implication of which is that the wrench intensity and joint effort vectors are uniquely defined by the system configuration variables, $\mathbf{q}$ and $\boldsymbol{\theta}$, so C-space need not be augmented. Also, since each contact corresponds to a geometric C-function in $n_q + n_\theta$ variables, the dimension of noncompliant FS-cells is n_θ. The class of compliant FS-cells is characterized by the matrix $\mathbf{W}_n$ being full rank and possessing a nontrivial null space. This implies the maintenance of $n_q + \eta$ contacts which requires active compliant control. This can be accomplished by effort-controlling an appropriate subset of the system's joints. In this case, C-space is augmented with the elements of the joint effort vector, so the dimension of C-space grows to $n_q + 2n_\theta$. Fortunately, the numbers of geometric and physical C-function equations defining FS-cells also grow to $n_q + \eta$ and $n_\theta - \eta$, respectively. Therefore, once again, the dimension of FS-cells is n_θ despite the augmentation of C-space. Physically, this result corresponds to the well-known fact that in rigid body systems, the position and effort of a joint cannot be controlled simultaneously.

Figure 2 shows a two-dimensional FS-cell corresponding to the four-contact CF of the initial grasp shown in Figure 1. Manipulation maintaining the CF of the initial grasp (see Figure 1 would require compliant control. This could be accomplished by controlling the right-hand finger's torque to lie between the bounds (shown in bold solid lines) while the other finger was position-controlled. Note that the upper bound goes to infinity, but was truncated at the maximum torque that our system could apply. Where the upper bound is finite, applying a greater torque would cause a palm contact to break, so the corresponding CF would not be maintained. Where the bound is infinite, the geometry of the contacts is such that the workpiece may be squeezed infinitely tightly without breaking any contacts. This is **the** fundamental characteristic of workpiece envelopment (discussed further below). The zero-valued lower bound alludes to two facts: the weight of the workpiece passes through the edge of contact on the palm and applying a negative torque would cause the right-hand finger to accelerate away from the workpiece.

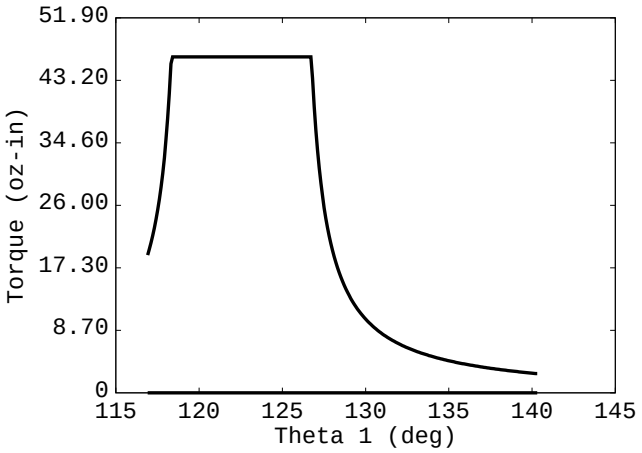

Figure 2: Compliant FS-cell for initial CF.

3.1.3 Envelopment: Form Closure

Envelopment is equivalent to the purely geometric condition of form closure, which was defined by Reuleaux in 1876 as follows:

Definition: Form Closure: A fixed set of contacts on a rigid body is said to exhibit *form closure* if the body's equilibrium is maintained despite the application of any possible externally applied wrench.

Since form closure is a geometric condition, its existence can be determined by considering $\mathbf{W}_n$. The necessary and sufficient conditions for form closure are that the rank of $\mathbf{W}_n$ be n_q and that the positive vector $\mathbf{k}$ exist such that the product $\mathbf{W}_{nI}{}^{-1}\mathbf{W}_{nII}\ \mathbf{k}$ has strictly negative elements [12]. From these conditions, one can infer that n_c must be greater than n_q . Therefore, form closure can only exist in regions of compliant FS-cells. Points satisfying the necessary and sufficient conditions can be written as follows:

$$\begin{aligned} \mathcal{FMC}^+ &= \{(\mathbf{q}\ ,\boldsymbol{\theta}\ ,\boldsymbol{\tau}\ ) \mid \bigwedge \mathbf{k}\ > \mathbf{0} \bigwedge d > 0 \\ &\quad \bigwedge -Adj(\mathbf{W}_{nI}\ )\mathbf{W}_{nII}\ \mathbf{k}\ > \mathbf{0}\} \qquad (19) \end{aligned}$$

$$\mathcal{FMC}^{-} = \{(\mathbf{q}\ ,\boldsymbol{\theta}\ ,\boldsymbol{\tau}\ ) \mid \bigwedge \mathbf{k}\ > \mathbf{0} \bigwedge d < 0 \bigwedge -Adj(\mathbf{W}_{nI}\ )\mathbf{W}_{nII}\ \mathbf{k}\ < \mathbf{0}\} \quad (20)$$

Intersecting the sets $\mathcal{FMC}^{+}$ and $\mathcal{FMC}^{-}$ with $\mathcal{FS}$ yields the subset of $\mathcal{FS}$ in which the workpiece is enveloped. The primary drawback of form closure configurations is that the relatively large numbers of contacts reduces the mobility of the workpiece. However, this can help reduce planning time since the the dimensions of the corresponding CF-cells are relatively small.

3.1.4 Generation of Joint Trajectories

Once a path through the FS-cell connectivity graph has been found, a path through each FS-cell must be found. Since FS-cells are not convex sets, geodesic segments connecting entry and exit points in the FS-cells are not guaranteed to yield feasible plans. However this can be overcome by employing slightly modified versions of Lumelsky's "Bug" algorithms [5].

3.2 Planning: Phase 2

Manipulation plans determined in Phase 1 assume that all contacts slide and by construction satisfy the applicable kinematic constraints, (1) and (2), at every point along the joint space path. However, the execution of a frictionless quasistatic plan in the presence of friction raises the question, "Does the quasistatic motion model (equations (1)-(5)) admit solutions with rolling contacts somewhere along the planned path?" If the answer is "Yes," then execution of the planned control trajectories may not produce the desired manipulation. Therefore, we must determine conditions under which the answer is "No" by checking the quasistatic feasibility of all 3^{n_c} possible modes of motion [14].

Our motion model is quasistatic, but, unfortunately, mode-of-motion switching is an inherently dynamic event. Joint and object velocities and wrench intensities undergo discontinuous changes. Thus one would be tempted to include dynamic and impact effects. However, while the quasistatic motion model may not be the best model for predicting switching between modes, we found it a reasonable indicator and we were able to use it to prevent rolling based upon the following logic. Mode-of-motion switching is viewed as an impact which gives rise to transients in control efforts and contact forces that are assumed to attenuate quickly (i.e., before the system configuration has changed appreciably). Also, because the system is moving slowly, dynamic considerations may not yield significantly different predictions of mode-of-motion switching. Therefore, in a given configuration, if only the planned mode of motion is feasible, then that mode will probably persist otherwise mode-of-motion switching is possible. Thus the conditions for the feasibility of mode-of-motion switching at a point on the planned path are:

1. The potential new mode of motion must be kinematically feasible given the current joint velocities of the position-controlled subset of the joints.

2. Equilibrium of both the planned mode of motion and the hypothesized new mode must be simultaneously feasible given the current of joint efforts applied by the subset of effort-controlled joints.

If these conditions are not met, then mode-of-motion switching results in a system state that is dynamic, thereby violating the quasistatic model[2].

The two mode-of-motion switching conditions restrict the set of potential new modes to those with the same number of kinematic constraints as the planned motion. Modes with more kinematic constraints have overdetermined systems of applicable kinematic equations (1), because too many of the elements of the joint velocity vector are specified by the plan. Modes with fewer kinematic constraints violate the equilibrium equations (3) and (4), because too many elements of the joint effort vector are specified. Therefore only modes of motion for which $2n_{R_2} + n_{S_2} = n_{S_1}$ (with one exception discussed below) need be considered. The scalar n_{S_1} is the number of sliding contacts in the planned mode of motion and n_{R_2} and n_{S_2} are the numbers of rolling and sliding contacts in the potential new mode of motion. This relationship between the numbers of sliding and rolling contacts substantially reduces the number of modes of motion that must be considered. For example, for cases with 3 and 4 contacts, the numbers of modes reduces from 27 to 7 and from 81 to 18, respectively.

Figure 3 shows (in bold solid lines) the upper and lower torque bounds corresponding to all the CF-cells of the complete manipulation plan shown in Figure 5 (as a piecewise smooth solid curve) [3]. The regions between the bounds are a series of connected FS-cells defined in subsubsection 3.1.2. The dashed curves are the FS-cells modified to include friction effects. The horizontal axis has units of distance along the joint space path. The FS-cells were not plotted against a joint angle, since they would overlap and be difficult to interpret.

Consider the frictionless bounds in Figure 3. From distance 0 to 234, the bounds are those shown in Figure 2. At 235, the workpiece has been translated leftward until the lower left vertex of the workpiece contacts the left finger (it still contacts the palm). The workpiece instantaneously gains form closure and both torque bounds exhibit jump discontinuities. Moving beyond 235, the workpiece rotates clockwise maintaining two contacts on the left finger, one on the palm,

[2] These conditions do not allow the prediction of potential jamming, because when the system jams, $\dot{\mathbf{q}}$ and $\dot{\theta}$ become zero, violating Condition 1. In general jamming is important. However, in the specific application discussed below, the coefficient of friction was small enough so that jamming never occurred. Therefore, we will not discuss it further here.

[3] This is the same path that was discussed in [11] before formalizing the concept of FS-cells

and one on the right finger. At 520, a new contact occurs on the palm. The object then translates to the left, breaking the distal contact on the left finger. The lower torque bound returns to zero, because the weight of the workpiece passes through the edge contact on the palm. As the workpiece slides leftward toward its goal, form closure is again achieved.

The bold dashed lines in Figure 3 are the torque bounds modified for Coulomb friction. The same coefficient, 0.1, was assumed at all contact points. The qualitative features of curves are quite similar to those of the frictionless case, however, there are two distinctive features. First, the discontinuity at 273 is the point at which the direction of sliding at one contact reversed. This reversal caused a discontinuity in $\mathbf{W}_A$ which is used in the computation of the torque bounds. Second, in the short interval beginning at 520 where the frictionless workpiece lost form closure, the frictional workpiece did not. This is because in the frictional case, sliding has the same effect as tilting the contact normals and in this case the tilting caused frictional form closure.

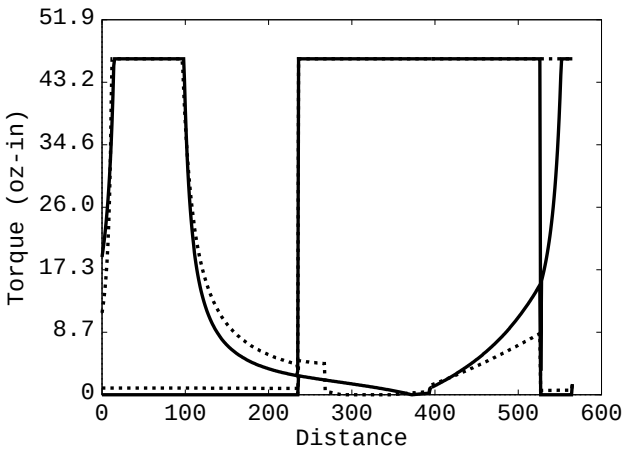

Figure 3: FS-cells modified by friction.

Only in the initial portion (from 0 to 234) of the manipulation plan was rolling contact a potential problem. The bold dashed curves shown in Figure 4 are the same torque bounds shown as bold dashed curves in the previous figure. The solid curve rising gently between the bounds is the upper bound for the potential mode of motion with rolling contact. The lower bound is zero. This plot suggests that the applied torque during manipulation be chosen above the solid curve. When this was done, the manipulation task progressed according to the frictionless plan. If not, rolling at the left-most palm contact was observed. However, it was not clear whether mode-of-motion switching occurred in the region where both the planned and rolling modes of motion were feasible, or in the region where only the rolling mode was feasible.

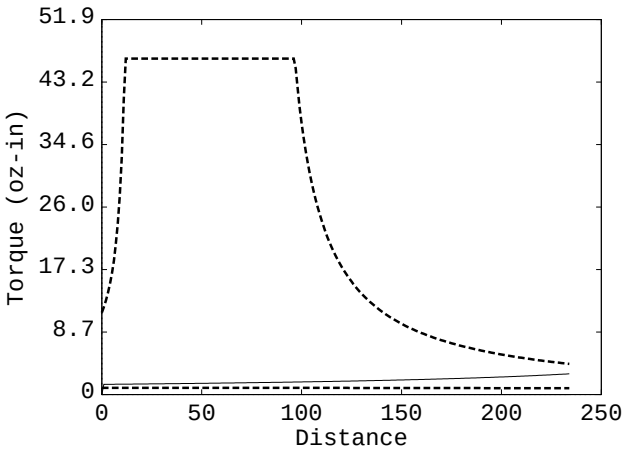

Figure 4: Torque bounds for four sliding contacts and for one rolling, two sliding, and one breaking.

4 Experimental Results

A scale model of the system depicted in Figure 1 was built with teflon-coated links. The fingers were directly driven by d.c. motors whose joint angles were sensed by potentiometers. Each motor could operate in either a closed-loop position-control mode or an open-loop effort-control mode; both operated at $100Hz$. The controllers were implemented on an 80486-based personal computer running LynxOS. Each control mode for each motor was implemented in C as a thread with one thread per finger active during any given control cycle. When the planned number of applicable kinematic constraints changed, the set of active control threads was changed accordingly. Compliant motions maintaining four contacts were implemented by position-controlling the right joint while torque-controlling the other.

Figure 5 shows the piecewise smooth path in joint space that was executed to achieve the desired grasp of the workpiece (see Figure 1). The path corresponds to compliant moves with four and five contacts. The five-contact CF-cells are the extreme upper-right and lower-left corners in the plot. The four-contact CF-cells are the smooth curve segments connecting them. The slope discontinuities correspond to configurations where a vertex of a finger slides across a vertex of the workpiece. At the lower left corner, the path appears to double back. It does not; the curves entering and leaving the corner correspond to distinct CF's. The noisy curve overlaying the piecewise smooth curve is a plot of the joint angles sensed during execution of the task. The plots shows relatively good agreement between the theoretical and actual joint space paths except near the goal. The primary cause of this discrepancy was dynamic effects arising during tipping. These effects could be corrected by increasing the gains of the controllers and increasing the task execution time, which for the plot below was approximately 5sec.

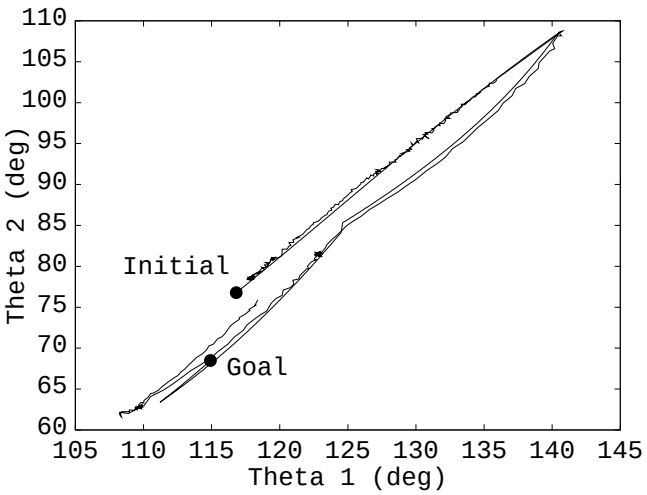

Figure 5: Planned and executed joint-space paths.

5 Conclusions

First-Order stability cells, or FS-cells, are regions of an augmented C-space in which a frictionless workpiece can be manipulated while maintaining stable equilibrium. All FS-cells, regardless of whether they correspond to noncompliant or compliant manipulation, have dimension n_θ . This is a welcome result from the perspective of manipulation planning, since the dimension of the corresponding C-space is $n_\theta + n_q$. The conditions for workpiece envelopment imply that envelopment can only occur with more than n_q contacts. Therefore its maintenance requires compliant control. The major disadvantage of FS-cells is the underlying assumption of no friction. However, it was demonstrated that the cells could be modified to guarantee successful execution in the presence of friction.

6 Acknowledgements

The authors would like to thank Drs. W. Newman and H. Kazerooni for their helpful suggestions regarding the construction of the prototype manipulation system.

This research was supported in part by the National Science Foundation through grant numbers MSS-8909678 and CDA-9115123, NASA Johnson Space Center through the Universities' Space Automation and Robotics Consortium contract number 28920-32525, and the Texas Advanced Technology Program grant number 32134-71120. Any findings, conclusions, or recommendations expressed herein are those of the authors and do not necessarily reflect the views of the funding agencies.

References

[1] D. L. Brock. Enhancing the dexterity of a robot hand using controlled slip. Master's thesis, MIT Department of Mechanical Engineering, 1987.

[2] R. S. Desai and R. A. Volz. Identification and verification of termination conditions in fine motion in presence of sensor errors and geometric uncertainties. In *Proceedings, IEEE International Conference on Robotics and Automation*, pages 800–807, May 1989.

[3] R. S. Fearing. Simplified grasping and manipulation with dextrous robot hands. *IEEE Journal of Robotics and Automation*, RA-2(4):188–195, December 1986.

[4] J.-C. Latombe. *Robot Motion Planning*. Kluwer Academic Publishers, 1991.

[5] V. Lumelsky and A. Stepanov. Dynamic path planning for a mobile automaton with limited information on the environment. *IEEE Transactions on Automatic Control*, AC31(11), November 1986.

[6] K. M. Lynch. The mechanics of fine manipulation by pushing. In *Proceedings, IEEE International Conference on Robotics and Automation*, pages 2269–2276, May 1992.

[7] M. T. Mason and J. K. Salisbury. *Robot Hands and the Mechanics of Manipulation*. mitp, Cambridge, Massachusetts, 1985.

[8] M. A. Peshkin and A. C. Sanderson. The motion of a pushed, sliding workpiece. *IEEE Journal of Robotics and Automation*, 4(6):569–598, December 1988.

[9] J. K. Salisbury. Whole-arm manipulation. In *Robotics Research: The Fourth International Symposium*, August 1987. Santa Cruz, CA.

[10] J. C. Trinkle, J. M. Abel, and R. P. Paul. An investigation of frictionless enveloping grasping in the plane. *International Journal of Robotics Research*, 7(3):33–51, June 1988.

[11] J. C. Trinkle and J. J. Hunter. A framework for planning dexterous manipulation. In *Proceedings, IEEE International Conference on Robotics and Automation*, pages 1245–1251, April 1991.

[12] J.C. Trinkle. On the stability and instantaneous velocity of grasped frictionless objects. *IEEE Transactions on Robotics and Automation*, 8(5):560–572, October 1992.

[13] J.C. Trinkle, A.O. Farahat, and P.F. Stiller. First-order stability cells for frictionless rigid body systems. *IEEE Transactions on Robotics and Automation*, January 1993. submitted.

[14] J.C. Trinkle and D.C. Zeng. Planar quasistatic motion of a lamina with uncertain contact friction. In *Proceedings, IEEE International Conference on Intelligent Robots and Systems*, pages 1642–1649, 1992.